

# Flux Growth of Highly Crystalline Photocatalytic BaTiO<sub>3</sub> Particle Layers on Porous Titanium Sponge Substrate and Insights into the Formation Mechanism

Q Wang<sup>1</sup> and B Li<sup>1\*</sup>

<sup>1</sup> School of Mechanical and Power Engineering, East China University of Science and Technology, 130 Meilong Road, Shanghai 200237, P. R. China

\* Corresponding author. Tel: +86-21-64252601; E-mail: bingli@ecust.edu.cn.

**Abstract.** A unique architecture of idiomorphic and highly crystalline BaTiO<sub>3</sub> particle layers directly grown on a porous titanium sponge substrate was successfully achieved for the first time using a facile molten salt method at a relatively low temperature of 700 °C. Specifically, the low-melting KCl-NaCl eutectic salts and barium hydroxide octahydrate were employed as the reaction medium and barium source, respectively. Powder X-ray diffraction (XRD), scanning electron microscopy (SEM), Energy dispersive X-ray spectroscopy (EDS), transmission electron microscopy (TEM), high-resolution transmission electron microscopy (HRTEM) and UV-vis diffuse reflectance spectrophotometry were used to characterize the structure, morphology and optical property of the obtained samples. The results revealed that the flux-grown tetragonal BaTiO<sub>3</sub> products had well-defined and uniform morphology with an average size of 300 nm and a band gap of ~3.16 eV. Based on XRD, EDS, SEM, and TEM, the possible formation mechanism responsible for the well-developed architecture of BaTiO<sub>3</sub> particle layers was proposed and discussed. Furthermore, the photocatalytic activity of the flux-grown BaTiO<sub>3</sub> products for organic pollutant degradation under simulated sunlight irradiation was also investigated.

## 1. Introduction

Semiconductor photocatalysis has attracted extensive attention due to its potential applications in photodegradation of organic pollutants, H<sub>2</sub> generation from water splitting, CO<sub>2</sub> reduction into hydrocarbon fuels and the removal of heavy metal ions, which greatly contributes to the solution of worldwide problems of energy crisis and environmental pollution[1,2,3]. It is well-known that the development of highly efficient, cost-effective and stable photocatalysts is crucial for the further advancement and large-scale practical applications of photocatalytic technique. During the past few decades, tremendous efforts have been devoted to developing new-type photocatalytic materials, including metal oxides (TiO<sub>2</sub>, ZnO, etc.), metal sulfides (CdS, MoS<sub>2</sub>, etc.), titanates (SrTiO<sub>3</sub>, BaTiO<sub>3</sub>, etc.), vanadates (Ag<sub>3</sub>VO<sub>4</sub>, BiVO<sub>4</sub>, etc.), tungstates (ZnWO<sub>4</sub>, CdWO<sub>4</sub>, etc.), metal phosphates (Ag<sub>3</sub>PO<sub>4</sub>, BiPO<sub>4</sub>, etc.), niobates (NaNbO<sub>3</sub>, Bi<sub>5</sub>Nb<sub>3</sub>O<sub>15</sub>, etc.), metal-free semiconductor (g-C<sub>3</sub>N<sub>4</sub>), and the related composite photocatalysts[4,5,6].

However, most photocatalysts still suffer from the shortcomings such as high recombination rate of photogenerated electron-hole pairs, small specific surface area and low sunlight utilization efficiency. Moreover, the separation and recovery of nanophotocatalysts from the treated effluent should be also concerned for practical industrial application[7,8]. Therefore, developing novel and highly efficient



photocatalysts with rational structural design is still a challenging task for the applications of photocatalysis in solar energy utilization and environmental remediation.

In this work, a unique architecture of idiomorphic and highly crystalline BaTiO<sub>3</sub> particle layers directly grown on porous Ti sponge substrate was prepared for the first time by the facile molten salt method in KCl-NaCl flux at 700 °C. On one hand, the porous structure of Ti sponge is beneficial to improve the adsorption properties of the BaTiO<sub>3</sub> products and then facilitate the photocatalytic reactions. Moreover, it is reported that the band bending nature of tetragonal BaTiO<sub>3</sub> ferroelectric material can inhibit the recombination of charge carriers, thereby contributing to the enhancement of its photocatalytic performance[8,9,10]. On the other hand, the flux-grown BaTiO<sub>3</sub> photocatalysts attached on the Ti sponge can be easily reclaimed from the environment without secondary pollution. Based on the characterization results including XRD, SEM, EDS and TEM, the corresponding formation mechanism of flux-grown BaTiO<sub>3</sub> particle layers on porous Ti sponge can be demonstrated clearly under the controlled experimental conditions, which can provide a new approach to fabrication of other highly efficient photocatalysts for the practical energy and environmental applications.

## 2. Experimental

In a typical procedure, the porous Ti sponge materials were ultrasonically cleaned in dilute hydrochloric acid, deionized water, acetone and ethanol in sequence and dried in air. Afterwards, Ti sponge and Ba(OH)<sub>2</sub>·8H<sub>2</sub>O were ground homogenously with NaCl-KCl eutectic salts (50 mol% NaCl + 50 mol% KCl) at a molar ratio of 1: 1: 20, and then transferred into a corundum crucible sealed with a lid. Subsequently, the mixture was calcined at 700°C in an electric furnace, and then cooled naturally to room temperature. The products were repeatedly washed with warm deionized water to remove residual salts, and finally dried at 90°C overnight. According to the holding time (1 h, 4 h, 8 h and 12 h), the obtained samples were denoted as BTO-1, BTO-2, BTO-3 and BTO-4, respectively.

The flux-grown samples were systematically characterized by XRD (Rigaku D/MAX 2550 VB/PC), SEM (Hitachi S-3400N), EDS (EDAX, Genesis XM2), TEM/HRTEM (JEOL JEM-2100), UV-vis diffuse reflectance spectrophotometry (Varian Cary 500 spectrophotometer). The photocatalytic activity of the obtained samples was evaluated by photodegradation of a 50 mL aqueous methyl orange (MO, 10 mgL<sup>-1</sup>) solution in the presence of 50 mg sample under simulated sunlight irradiation using a 300 W Xe lamp ( $\lambda > 300\text{nm}$ , PLS-SXE300) at room temperature. Prior to light irradiation, the suspension was magnetically stirred in dark until absorption-desorption equilibrium. The change of characteristic absorption of MO solution at  $\lambda = 465\text{ nm}$  corresponding to its concentration was monitored on the Varian Cary 500 spectrophotometer to evaluate the photocatalytic activity.

## 3. Results and Discussion

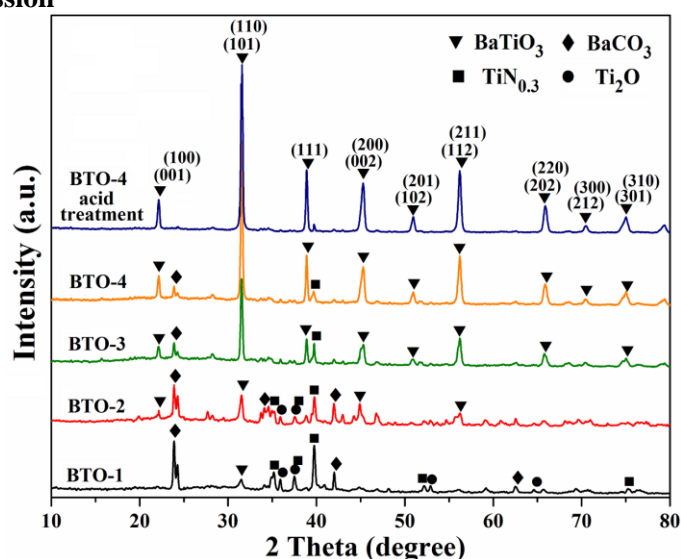
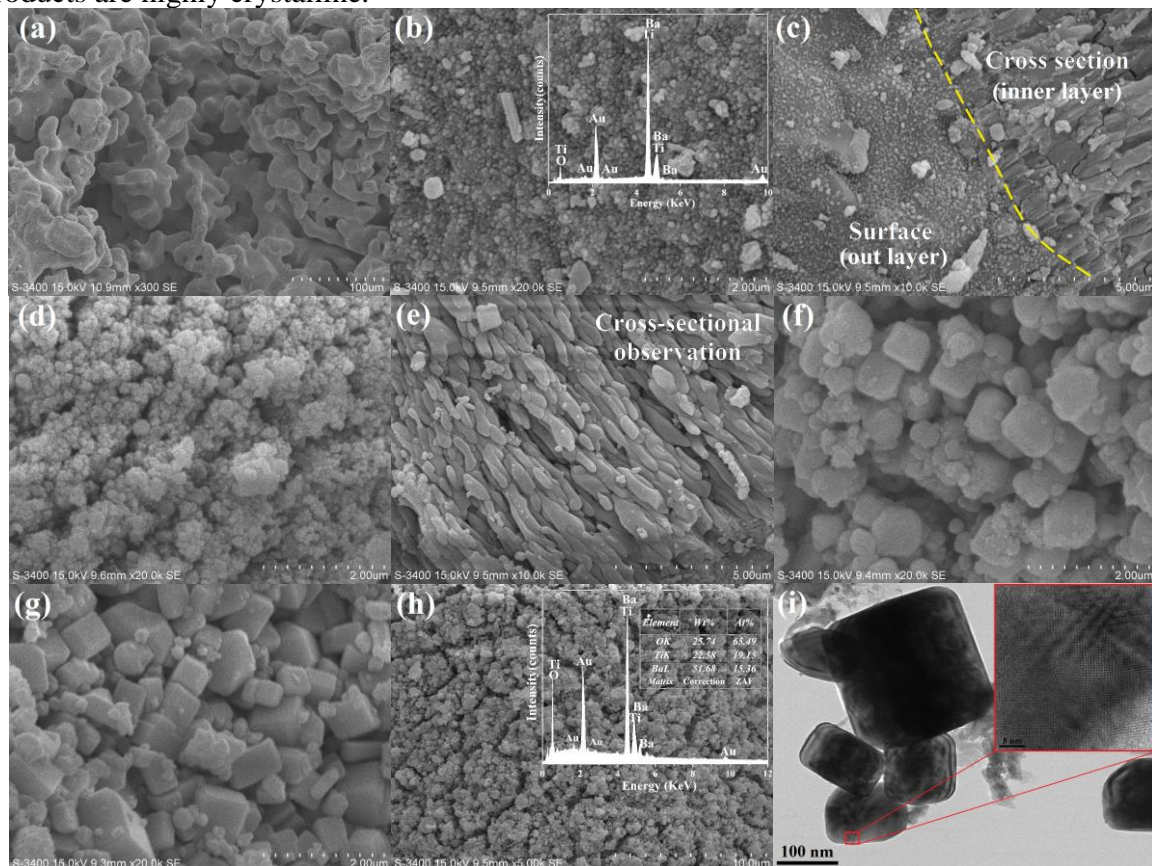


Figure 1. XRD patterns of the as-synthesized samples.

As shown in Figure 1, XRD patterns of the obtained samples reveal that BTO-1 is mainly composed of  $\text{BaCO}_3$  (JCPDS Card NO. 05-0378),  $\text{TiN}_{0.3}$  (JCPDS Card NO. 41-1352),  $\text{Ti}_2\text{O}$  (JCPDS Card NO. 65-5293), and tetragonal  $\text{BaTiO}_3$  (JCPDS Card NO. 05-0626), but the amount of obtained  $\text{BaTiO}_3$  phase is relatively low, which can be attributed to the primary process of the formation of Ti-rich  $\text{TiN}_{0.3}$  and  $\text{Ti}_2\text{O}$  layers on Ti substrate during limited calcination time. Obviously, with the increasing of calcination time, the amount of  $\text{BaCO}_3$ ,  $\text{TiN}_{0.3}$  and  $\text{Ti}_2\text{O}$  decrease gradually, while the amount of  $\text{BaTiO}_3$  increase obviously. Meanwhile, the enhancement of diffraction peaks due to  $\text{BaTiO}_3$  can suggest the increase in the degree of grain growth and crystallinity of the flux-grown  $\text{BaTiO}_3$  crystals. When the calcination time reached 12 h, a large amount of tetragonal  $\text{BaTiO}_3$  phase was obtained, although it coexisted with certain unreacted  $\text{BaCO}_3$  (which could be easily removed by an acid treatment) and  $\text{TiN}_{0.3}$ . Moreover, the sharp and intense peaks indicate the flux-grown  $\text{BaTiO}_3$  products are highly crystalline.



**Figure 2.** Typical SEM images and EDS spectra (inset) of the samples: (a) Ti sponge (b, c) BTO-1, (d, e) BTO-2, (f) BTO-3, (g, h) BTO-4 and (i) TEM (inset, HRTEM) image of BTO-4.

Based on the XRD results, the SEM and TEM images in Figure 2 display clearly the formation process and morphology evolution of the flux-grown crystalline  $\text{BaTiO}_3$  particle layers on Ti sponge substrate. Figure 2a shows the Ti sponge has a porous structure with smooth surface. As shown in Figure 2b-c combined with the corresponding EDS analysis, the surface of BTO-1 is covered by compact Ti-rich  $\text{Ti}_2\text{O}$  nanoparticles (out layer) with an average size of  $\sim 100$  nm because no N element can be detected, and thus the inner layer consists of Ti-rich  $\text{TiN}_{0.3}$  phase. Here, no obvious  $\text{BaTiO}_3$  crystals can be found owing to their low amount. Figure 2d reveals that BTO-2 is composed of a large amount of amorphous and aggregated particles with the size less than 200 nm, while the  $\text{BaTiO}_3$  products can hardly be distinguished from the mixtures. Interestingly, as can be seen in Figure 2e, the cross-sectional SEM image shows that the inner layer of BTO-2 exhibits wormlike morphology, suggesting a remarkable structural evolution of inner layer in comparison with that of BTO-1. As for BTO-3,

well-crystallized  $\text{BaTiO}_3$  particles with a larger particle size can be seen in Figure 3f, which is in accordance with the XRD results. As shown in Figure 2g-h, BTO-4 has a unique architecture of well-defined  $\text{BaTiO}_3$  polyhedral crystal layers densely grown on Ti substrate. The small and amorphous particles can be assigned to the residual  $\text{BaCO}_3$ . In Figure 2i, TEM and HRTEM images reveal that the flux-grown  $\text{BaTiO}_3$  polyhedral crystals with the size of 100-300 nm are highly crystalline because no obvious defects can be observed in clear lattice fringes.

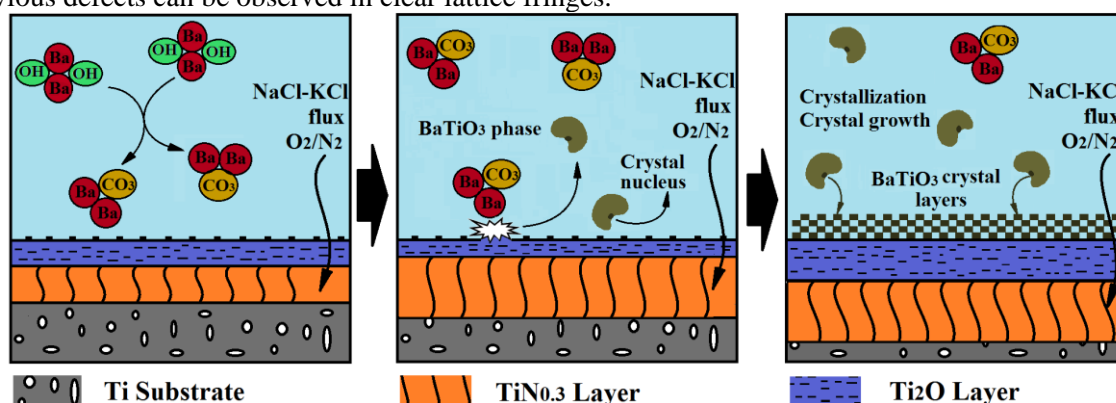


**Figure 3.** Schematic illustration of formation mechanism responsible for the well-developed  $\text{BaTiO}_3$  crystal layers grown on porous titanium sponge substrate.

Based on the above results and our previous studies[11,12], the formation mechanism responsible for the flux-grown  $\text{BaTiO}_3$  crystal layers on porous Ti sponge was proposed, as illustrated in Figure 3. The films of Ti-rich  $\text{Ti}_2\text{O}$  (out layer) and  $\text{TiN}_{0.3}$  (inner layer) were firstly formed on the surfaces of Ti sponge by the nitridation and oxidation reactions (i.e.,  $2\text{Ti} + 0.5\text{O}_2 \rightarrow \text{Ti}_2\text{O}$ ,  $\text{Ti} + 0.15\text{N}_2 \rightarrow \text{TiN}_{0.3}$ ) at the solid-liquid interface between Ti sponge and NaCl-KCl flux. Simultaneously,  $\text{Ba}(\text{OH})_2$  was transformed into  $\text{BaCO}_3$  by reacting with  $\text{CO}_2$  from the ambient. Generally speaking, the flux growth of well-defined polyhedral crystals can be ascribed to the dissolution and recrystallization process. With the increasing of calcination time, the  $\text{BaTiO}_3$  phase generated by the reaction (namely,  $\text{Ti}_2\text{O} + 1.5\text{O}_2 + 2\text{BaCO}_3 \rightarrow 2\text{BaTiO}_3 + 2\text{CO}_2\uparrow$ ) began to be dissolved in the NaCl-KCl flux and then  $\text{BaTiO}_3$  crystallites (i.e., crystal nucleus, serving as templates for further growth) would form and grow in-situ on  $\text{Ti}_2\text{O}$  layer with the increasing of solute concentration (i.e.,  $\text{BaTiO}_3$  phase). Meanwhile, the  $\text{TiN}_{0.3}$  was transformed into  $\text{Ti}_2\text{O}$  by reacting with atmospheric oxygen, which can further continually promote the generation of  $\text{BaTiO}_3$  phase. Therefore, according to the dissolution-precipitation mechanism, the precipitation of new-formed  $\text{BaTiO}_3$  on the aforementioned templates continued until the reactants were consumed completely, leading to the crystal growth and shape evaluation of the  $\text{BaTiO}_3$  crystals.

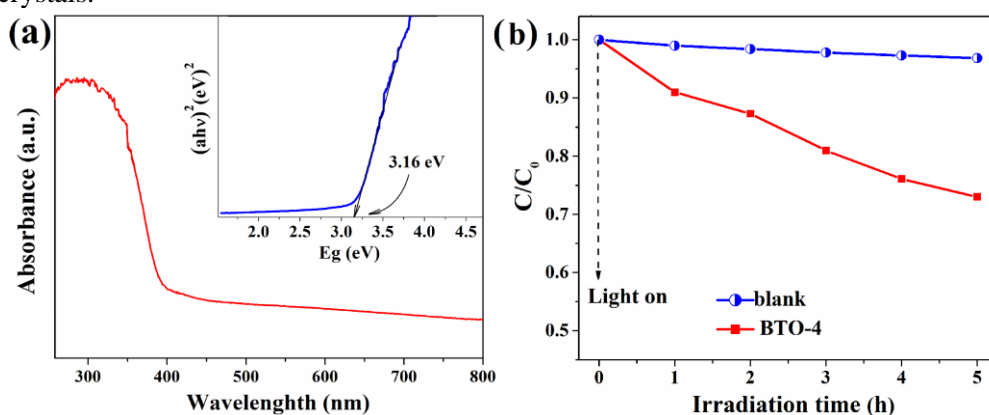


**Figure 4.** (a) UV-vis spectra of the sample BTO-4. Inset is the plot of  $(ah\nu)^2$  versus  $h\nu$  for calculating the  $E_g$ . (b) Photocatalytic degradation of MO over the flux-grown  $\text{BaTiO}_3$  products.

As shown in the UV-vis diffuse reflectance spectra (in Figure 4a), BTO-4 mainly absorb the UV light below about 400nm. The band gap energy ( $E_g$ ) of sample BTO-4 was calculated to be  $\sim 3.16$  eV,



according to the equation:  $\alpha h\nu = A(h\nu - E_g)^{1/2}$ , where  $\alpha$ ,  $h\nu$ , and  $A$  are the absorption coefficient, photon energy and a constant, respectively, which agrees with the previous reports[8,13]. Figure 4b displays the photocatalytic degradation of MO over the flux-grown BaTiO<sub>3</sub> products, revealing that the photocatalytic activity needs to be further improved to meet the requirements of practical environmental and energy applications, which is similar to the previous studies[8, 9, 13]. This can be mainly attributed to the high recombination rate of photogenerated electron-hole pairs and the weak visible-light harvesting ability of BaTiO<sub>3</sub>. Considering that the construction of semiconductor heterostructures has been intensely studied as an effective way to improve the photocatalytic activity, coupling the BaTiO<sub>3</sub> particles with other visible-light-driven photocatalysts (such as g-C<sub>3</sub>N<sub>4</sub>, MoS<sub>2</sub>, Ag<sub>3</sub>VO<sub>4</sub>, etc.) to enhance their photocatalytic properties will be carried out.

#### 4. Conclusion

In summary, a novel architecture of idiomorphic BaTiO<sub>3</sub> polyhedral crystal layers directly grown on a porous Ti sponge was successfully developed in KCl-NaCl flux at 700 °C. The flux-grown tetragonal BaTiO<sub>3</sub> products with well-defined shape and uniform morphology had a  $E_g$  of ~ 3.16 eV. The possible formation mechanism responsible for the well-formed BaTiO<sub>3</sub> particle layers was proposed based on the corresponding structural and morphological characterization. Finally, the simulated sunlight photocatalytic activity of the obtained BaTiO<sub>3</sub> products for MO degradation was also tested and discussed. Moreover, our work on further enhancing the photocatalytic performance of flux-grown BaTiO<sub>3</sub> photocatalyst is underway. Overall, this work offers a new strategy for designing other easily recycled photocatalytic materials with rational architectures favorable for practical application in solar energy conversion and environmental remediation.

#### 5. References

- [1] Hernández-Alonso M D, Fresno F, Suárez S and Coronado J M 2009 *Energy Environ. Sci.* **2** 1231
- [2] Tu W, Zhou Y and Zou Z 2014 *Adv. Mater.* **26** 4607
- [3] Li H, Zhou Y, Tu W, Ye J, Zou Z 2015 *Adv. Funct. Mater.* **25** 998
- [4] Zhao Z, Sun Y and Dong F 2015 *Nanoscale* **7** 15
- [5] Wang Q, Guo Q, Wang L and Li B 2016 *Dalton Trans.* **45** 17748
- [6] Wang H, Zhang L, Chen Z, Hu J, Li S, Wang Z, Liu J and Wang X 2014 *Chem. Soc. Rev.* **43** 5234
- [7] Akhundi A and Habibi-Yangjeh A 2016 *Mater. Chem. Phys.* **174** 59
- [8] Fan H, Li H, Liu B, Lu Y, Xie T and Wang D 2012 *ACS Appl. Mater. Interfaces* **4** 4853
- [9] Cui Y, Briscoe J and Dunn S 2013 *Chem. Mater.* **25** 4215
- [10] Kappadan S, Gebreab T W, Thomas S and Kalarikkal N 2016 *Mater. Sci. Semicon. Proc* **51** 42
- [11] Wang Q, Guo Q, Hu Y and Li B 2016 *CrystEngComm* **18** 6926
- [12] Wang Q, Guo Q and Li B 2015 *RSC Adv.* **5** 66086
- [13] Xian T, Yang H, Di L J and Dai J F 2015 *J Alloys Compd.* **622** 1098

#### Acknowledgments

This work was supported by National Natural Science Foundation of China ( No.51274102).